6-2017

Electromagnetic radio frequency heating in the pulsed electric current sintering (PECS) process

Yufei Liu
Clemson University, yufeil@clemson.edu

D. H. Liebenberg
Clemson University

Recommended Citation
Liu, Y., & Liebenberg, D. (2017). Electromagnetic radio frequency heating in the pulsed electric current sintering (PECS) process. MRS Communications, 7(2), 266-271. doi:10.1557/mrc.2017.35

Draft Feb. 1, 2017

ELECTROMAGNETIC RADIO FREQUENCY HEATING IN THE PULSED ELECTRIC CURRENT SINTERING (PECS) PROCESS

Yufei Liu and D. H. Liebenberg

Clemson University

ABSTRACT

Pulsed electric current sintering (PECS) offers rapid sintering of many materials compared to hot press sintering. Earlier studies (refs. 1, 2) have demonstrated that the term spark plasma sintering is misleading since neither sparks nor plasma formation occur in a typical apparatus such as Dr. Sinter ™. In reference 2 electromagnetic radio frequency (rf) emission during the pulsing current of the PECS was demonstrated and suggested as a physically relevant augmentation to the hot press sintering in addition to the current flow in the specimen. In this report the importance of rf emission in the sintering process is demonstrated and opportunities to further exploit this approach to improve the sintering process are suggested.

INTRODUCTION

Pulsed electric current sintering (PECS) as developed in the Dr. Sinter™ apparatus[3] has demonstrated faster and higher compaction of sintered specimens compared to the hot press technique. In part, this improvement is due to pulsed current flow through the specimen providing Joule heating and in part due to what has been called Spark Plasma Sintering. Spark plasma sintering (SPS) in the Dr. Sinter™ has been demonstrated[1,2] to exhibit neither sparks nor plasma. However in Ref. 2 the electromagnetic emission at radio frequencies (rf) of 10 kHz to 160 kHz was observed and suggested to be an additional difference to the hot press sintering technique. These two techniques are generally applicable to smaller specimens and microwave sintering has been developed for heating and sintering with electromagnetic radiation at tHz frequencies for larger samples[4]. Thus PECS represents an intermediate step between hot pressing and microwave sintering. This report extends the rf emission frequency measurement to above 600 kHz although the peak in the emission is 12 kHz or lower. To examine the influence of the electromagnetic radiation on the sintering process a technique is presented to limit the current through the specimen while providing the electromagnetic radiation to envelop the specimen. The electromagnetic radiation importance to the PECS process is demonstrated.

RF SPECTRUM ANALYSIS

The MDO 4104 B-6 Tektronix[2,5] spectrum analyzer was used together with the thermocouple antenna (TCa)[6] located inside the Dr. Sinter™ vacuum chamber and external to the die as seen in Fig. 1. The frequency range was expanded from the 10 kHz lower limit of the analyzer to 2 MHz. Fig. 2A (lower panel) shows the signal fades into noise at about 400-650 kHz. An additional measurement was made with the probe inserted through the die into the specimen of

Al_2O_3 and compared with the signal external to the die. A signal increase of ~15 dBm from -50 dB_M was measured corresponding to 3.2 μW[5]. Note that the TCa probe size is about 0.2mm.

An improved measurement of the current pulse was obtained using a Hall probe[7] clamp around the current leads into the vacuum chamber. The output voltage is related to the current by the manufacture's calibration. Thus, in Fig. 2A the red curves in the upper and middle panels are the Hall probe voltage independently and simultaneously recorded and compared to the thermocouple antenna (TCa) pulses (in dark blue). The Hall probe provides capture at < 10 μs so the rise time in the selected region (blue bar in Fig. 2A) can be sampled with the TCa to capture the frequency spectrum in this pulse region of onset of the current pulse and peak (lower panel light blue curve) of Fig. 2A. The TCa measured peak rf emission at 12 kHz is -49.9 dB_M or 10 nW. Fig. 2B shows the spectrum obtained during the pulse peak and initial turn off region (blue bar) and the rf spectrum signal from the TCa is reduced from 10 nW to 0.3 pW at the peak frequency of 12 kHz. This is consistent with the earlier measurements with the TCa indicating a maximum response during the pulse rise (blue curve in the upper and middle panels of Fig. 2).

RF EMISSION IMPORTANCE IN SINTERING

Normal operation of the PECS process

In the normal operation of the Dr. Sinter™ the current flows through the specimen and the electromagnetic wave rf emission occurs within the specimen and the punch and die. This is different from hot press sintering where thermal heating is conducted to the specimen. In PECS there is also thermal radiation and conductive heating from the surrounding punch and die that contributes at higher temperatures. As determined above and shown in Fig. 2 A/B rf emission occurs predominantly in the initial rise of each current-on pulse. Much lower rf emission is measured during the pulse peak and decay.

Modification of the PECS process to demonstrate the importance of rf emission

In order to differentiate the electromagnetic wave rf emission importance in the PECS process pre-sintered disks of the electrical insulator Al_2O_3 (300 mesh Alfa Aesar) were separately sintered and installed above and below the selected material specimen. These disks with the 12 mm diameter of the punch and thickness each of 3 mm, restrict the current flow through the specimen and thus restrict both the internal rf emission and Joule heating. However, the electromagnetic wave rf emission from the pulsed current in the die envelops the specimen enhancing the proportion of energy to the specimen from the rf emission. Thermal and radiative heating from the die will also transmit to the specimen.

Nickel (Ni) and manganese (Mn) were selected for the specimen materials and the sintered disks had a thickness of about 6 mm. These materials, Mn (325 mesh 99.99% Alfa Aesar) and Ni (100 mesh 99.9% Alfa Aesar), form an interesting pair as seen from properties listed in Table I. The Mn has a higher electrical resistance and lower thermal conductivity than Ni, in each parameter by more than an order of magnitude. The melting temperatures are high in both materials and

the molar specific heats are similar. Also the Al_2O_3 disks have a very high electrical resistance and an intermediate thermal conductivity to Mn and Ni.

The temperature is measured with a thermocouple (TC) inserted in the die. A temperature-in-the-die vs time profile was chosen, after trials, to provide for a long sequence (12/2 pulse on/off) of pulses at a low current (100A) of the Dr. Sinter™ and to provide a short current increase to produce a temperature well below the normal sintering temperatures and the melting temperatures of these specimens. An additional 10 min at 100 A current followed. A low force on the specimen, 49 MPa (setting of 6 on Dr.Sinter™), was used to further delineate the effect of the rf emission on the densification process.

RESULTS

An example of two runs for Ni (2.5 gm) without disks is shown in Fig. 3 where the initial current is 100 A set for 10 min, then a current of 300 A is set for 1 min, and a current of 100 A is set for an additional 10 min. Comparison of the two temperature profiles measured with the TC in the die shows the uniformity of the two runs. The maximum temperature is well below the melting and normal sintering temperatures. Current flow and rf emission occurs in the specimen and the die.

With the Al_2O_3 (~0.5 gm each) disks in place and a Ni specimen of similar size as in the no-disk case, Fig 4 compares two nickel runs each with and without disks. These disks isolate the same size specimen from direct pulsed current flow through the specimen. Thus there is no rf emission generated in the specimen. **The rf emission is only generated from the pulsed current flow in the die and this radiates into the specimen.** There will be thermal conduction and radiant heat transfer from the pulsed current heating of the die. The temperature is measured in the die. The area of the die compared to that of the punch is 1.33 so that reducing the current flow through the punch and specimen will divert current flow to the die and thus cause a faster and higher temperature rise recorded by the TC in the die. The greater temperature rise in the die when the current through the specimen is blocked is clearly seen in Fig. 4. A temperature rise after 10 min results in a greater than 100 ^oC increase for the disk blocked current through the specimen compared to the specimen only experiment. And after the one minute at 300 A current the difference between the experiments with and without disks is further increased by about 150 ^oC. Some variation of the temperature vs time profiles for the two runs with Al_2O_3 disks is likely due to variations in Al_2O_3 disk sintering.

For the Mn (2.0 gm) specimens similar results are obtained. The temperature measured in the die increases more rapidly when the current path through the punch and specimen is blocked by the electrically insulating Al_2O_3 disks as shown in Fig. 5. The temperature rise difference at the end of the 10 min pulsing at 100 A is about 50 ^oC between the disks and no disks case. The smaller temperature difference indicates that more energy is going into the Mn compared to the larger temperature rise in Ni. This comparison supports the case for greater rf emission heating in the Mn.

Both the Ni and Mn specimens with no disks have a temperature rise at the end of 10 min that is similar, to about 200 ^oC. The temperature rise in the die for Ni with disks after the 10 min current of 100 A is about 100 ^oC or twice that in Mn with disks (about 50 ^oC) and indicates that there is some shielding of the radiated rf emission by Ni due to its lower resistivity. The higher

thermal conductivity of Ni and the Al_2O_3 disks might be expected to reduce the die temperature due to thermal heat conduction compared to the Mn (of lower thermal conductivity) with disks but the rf shielding by Ni appears more important.

Comparison of the densification produced by the radiated rf emission for disks in place with the normal (without disks) sintering is determined from density measurements. The densities of the sintered specimens are listed in Table 2 for Mn and Ni. These densities were obtained with the Archimedes method in water. For less than full density there is the possibility of water or air bubbles in the pores reducing the accuracy of the measurement. Measurements of the dimensions for these disks as they come from the die also have a significant error, thus the densities must be considered as indicative and not definitive. The density of both Ni and Mn with no disks and with the same time and temperature protocol is about 90% of full density. The density for Mn isolated by the disks is also about 90%, while the density of Ni is significantly less, about 75%. This is consistent with the better absorption of radiated rf emission for the Mn than for the rf shielding that the Ni with lower resistivity provides. In the normal (no-disks) case for Ni, the pulsed current through the sample will generate rf in the Ni enhancing the densification.

X-ray diffraction measurements are shown in Table 2 for the Ni and Mn specimens. For Ni specimens, the FWHM of the peak corresponding to hkl=(011) shows that with the addition of the Al_2O_3 disks, the X-ray peaks become broader. The value of FWHM can be used to estimate the grain size in a solid, given by Scherrer equation[8]. Basically, the grain size is inversely proportional to the FWHM. Thus for Ni specimens, adding Al_2O_3 disks would lead to a lower densification, in agreement with the density values.

Similar results were obtained for Mn specimens. The hkl=(221) peak was selected. As shown in Table 2, for Mn with disks, both density and FWHM indicate that the specimens are less well sintered than in the case without disks, but better sintered than the Ni with disks.

DISCUSSION

The Al_2O_3 disks, top and bottom of the specimen, clearly limit the current pulses from passing through the specimen as demonstrated by the higher temperature rise in the die from additional Joule and rf emission heating in the die. The temperature difference measured in the die after about 10 min pulsing at 100 A shows a temperature rise of 100 ^oC greater when the Ni specimen is isolated from the current flow with the Al_2O_3 disks but not from the radiated rf emission generated in the surrounding die. For Mn the temperature rise is about one-half that and indicates that more energy is being lost from the die with the Mn specimen. This is consistent with the view that more radiated rf emission is being absorbed by the Mn that has about 7 times the resistivity of the Ni. And it suggests that the more than a factor of 10 higher thermal conductivity for Ni is less effective than the rf emission radiation in transferring energy to the Ni specimen with disks even though the Al_2O_3 disks also have a fairly high thermal conductivity. Comparing the Ni and Mn temperature rise when no disks are used, very similar values of 200 ^oC are measured in the die after the 10 min at 100 A current as both Joule and rf emission heating occur within the specimen in addition to the heat transferred and the rf emission radiated from the die.

As seen from Table 2 the densities measured are consistent with greater radiated rf absorption by the Mn with disks, resulting in a higher fractional density. A lower fractional density of the Ni with disks is consistent with rf shielding by the lower resistivity.

The X-ray FWHM data show a decrease of densification to about 90% for both Ni and Mn specimens compared to a normal sintering temperature and time. With Al_2O_3 disks in place the greater densification for Mn compared to Ni with the disks provides additional support for the greater electromagnetic radiation absorption by the Mn.

CONCLUSION

The electromagnetic radiation spectrum at radio frequencies from 10- 400 kHz was determined to occur from the steep onset rise of the current pulse in the PECS process. Isolating the pulsed current flow through specimens of Ni and Mn restricted the in-specimen rf emission and Joule heating. The rf emission radiated to the specimens from the pulsed current in the die in addition to thermal and radiative heating increased the fraction of energy to the specimen by the radiated rf emission from the die as determined by the temperature rise in the die. The densification for the sharply different resistivity and thermal conductivity between the Ni and Mn specimens agree with the measured temperature rise in the die and the absorption of the radiated electromagnetic rf emission from the die. The importance of this radio frequency emission in the sintering process of the PECS with the Dr. Sinter™ system has been demonstrated. These results suggest an opportunity to advance the sintering process by tuning and controlling the electromagnetic radiation in pulsed electric current sintering.

Fig. 1 Dr. Sinter specimen chamber. The thermocouple (TC) is located in the vacuum chamber and for die temperature measurements the TC is placed in a hole in the die. The TC is located in the vacuum chamber external to the die for measurements with the spectrum analyzer as an antenna (TCa).

Fig. 2A Upper panel; the Hall voltage (red) and the TC antenna (blue). Blue brackets select the region from the upper panel to the middle panel where the Hall voltage and TCa values are expanded. The blue bar selects the region for the rf signal capture shown in the lower panel. The lower panel displays the rf emission vs frequency as captured by the TCa. The lower frequency of 10 kHz has been shifted to near the center. The peak maximum at 12 kHz has a power level of 49.9 dB_M or 10 nW Ref. 5. Note the peak near 1 MHz corresponds to a local FM station.

Fig. 2B Colors and traces as shown in Fig. 2 A. The blue bar of the middle panel is shifted to include the pulse peak and initial shut off of the PECS current. From the peak at about 12 kHz in Fig. 2 a drop of 45 dBm is observed.

Fig. 3 Two PECS nickel specimens with no disks (2.5 gm each, 150 mesh fine powder, 99.96% pure). Temperatures measured in the die. Temperature profile from the current protocol: 10 min @ 100 A, 1 min @ 300 A, 10 min @ 100 A, cool in vacuum @ 0.0 A.

Fig. 4 Four PECS nickel specimens each with Ni as in Fig. 3 caption, two specimens without Al_2O_3 disks, red dots and blue squares, and two specimens with Al_2O_3 disks, top and bottom of the specimen, green and orange vertical and tilted triangles. The temperature is measured in the die and the current protocol is the same as in Fig. 3.

Fig. 5 Four PECS manganese specimens (2.0gm each, 325 mesh, 99.99% pure), two specimens without Al_2O_3 disks, red dots and blue squares, and two specimens with Al_2O_3 disks, top and bottom of the specimen, green and orange vertical and tilted triangles. The temperature is measured in the die and the current protocol is shown for the first 10 min pulsing on the expanded scale.

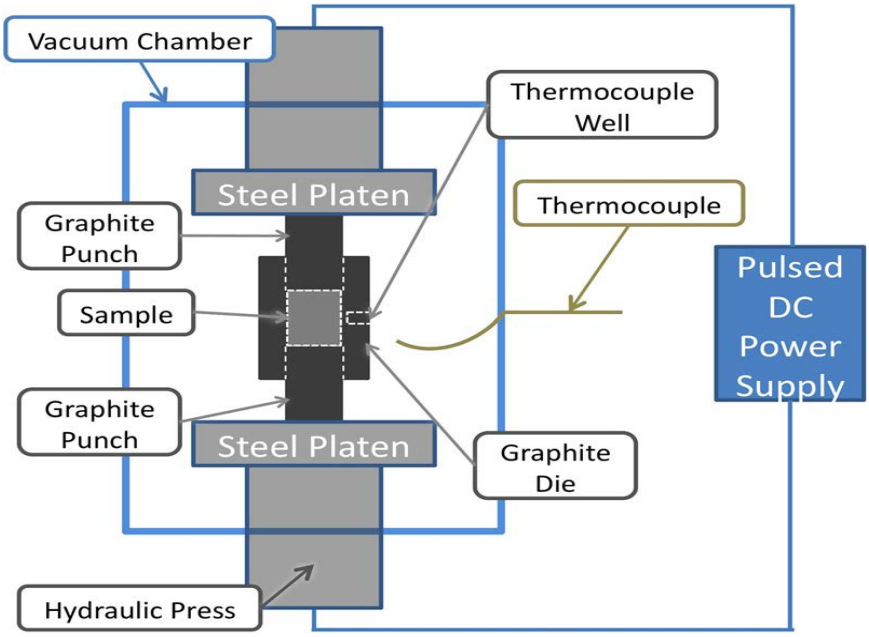

Fig. 1 Dr. Sinter specimen chamber. The thermocouple (TC) is located in the vacuum chamber and for die temperature measurements the TC is placed in a hole in the die. The TC is located in the vacuum chamber external to the die for measurements with the spectrum analyzer as an antenna (TCa).

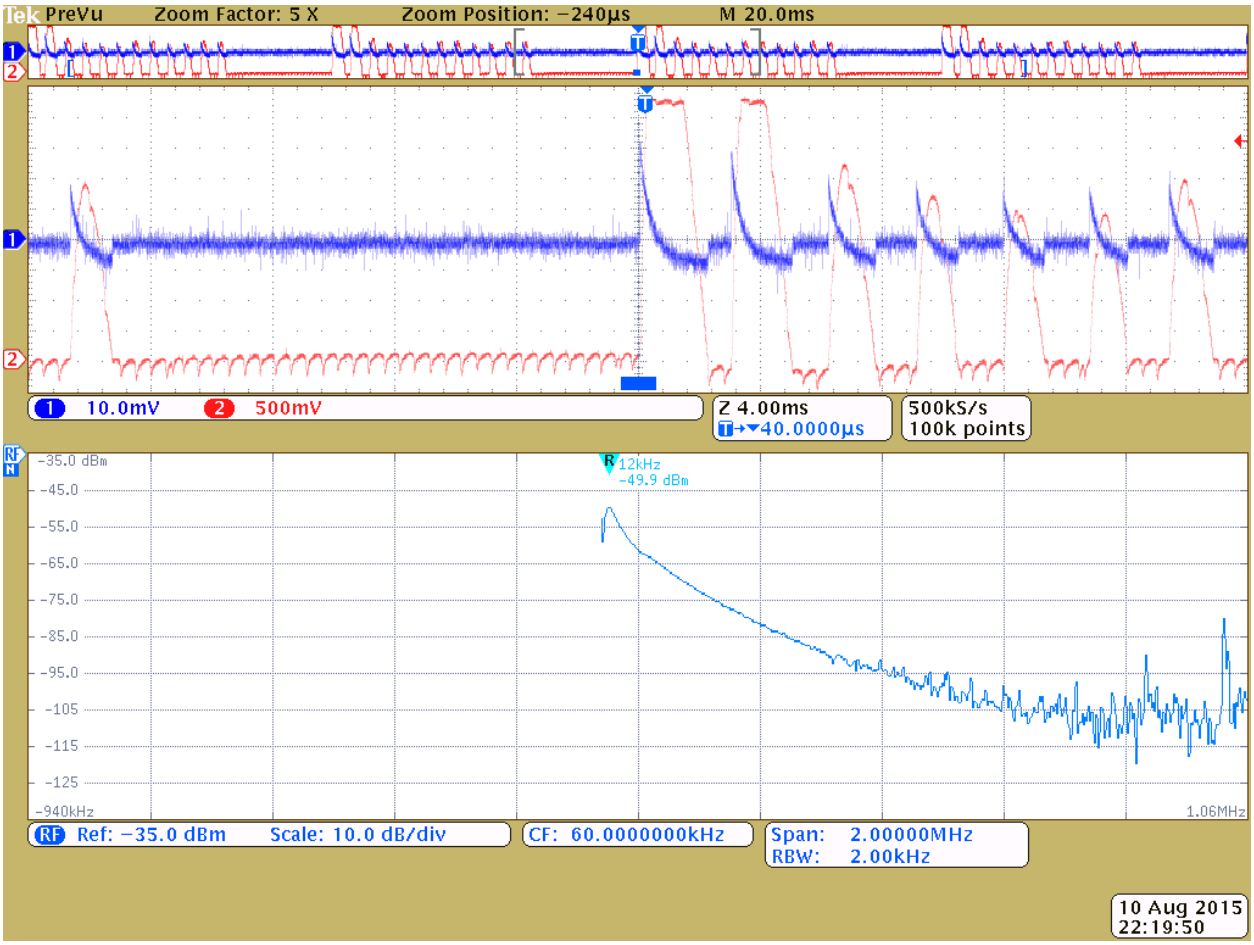

Fig. 2A Upper panel; the Hall voltage (red) and the TC antenna (blue). Blue brackets select the region from the upper panel to the middle panel where the Hall voltage and TCa values are expanded. The blue bar selects the region for the rf signal capture shown in the lower panel. The lower panel displays the rf emission vs frequency as captured by the TCa. The lower frequency of 10 kHz has been shifted to near the center. The peak maximum at 12 kHz has a power level of 49.9 dB_M or 10 nW Ref. 5. Note the peak near 1 MHz corresponds to a local FM station.

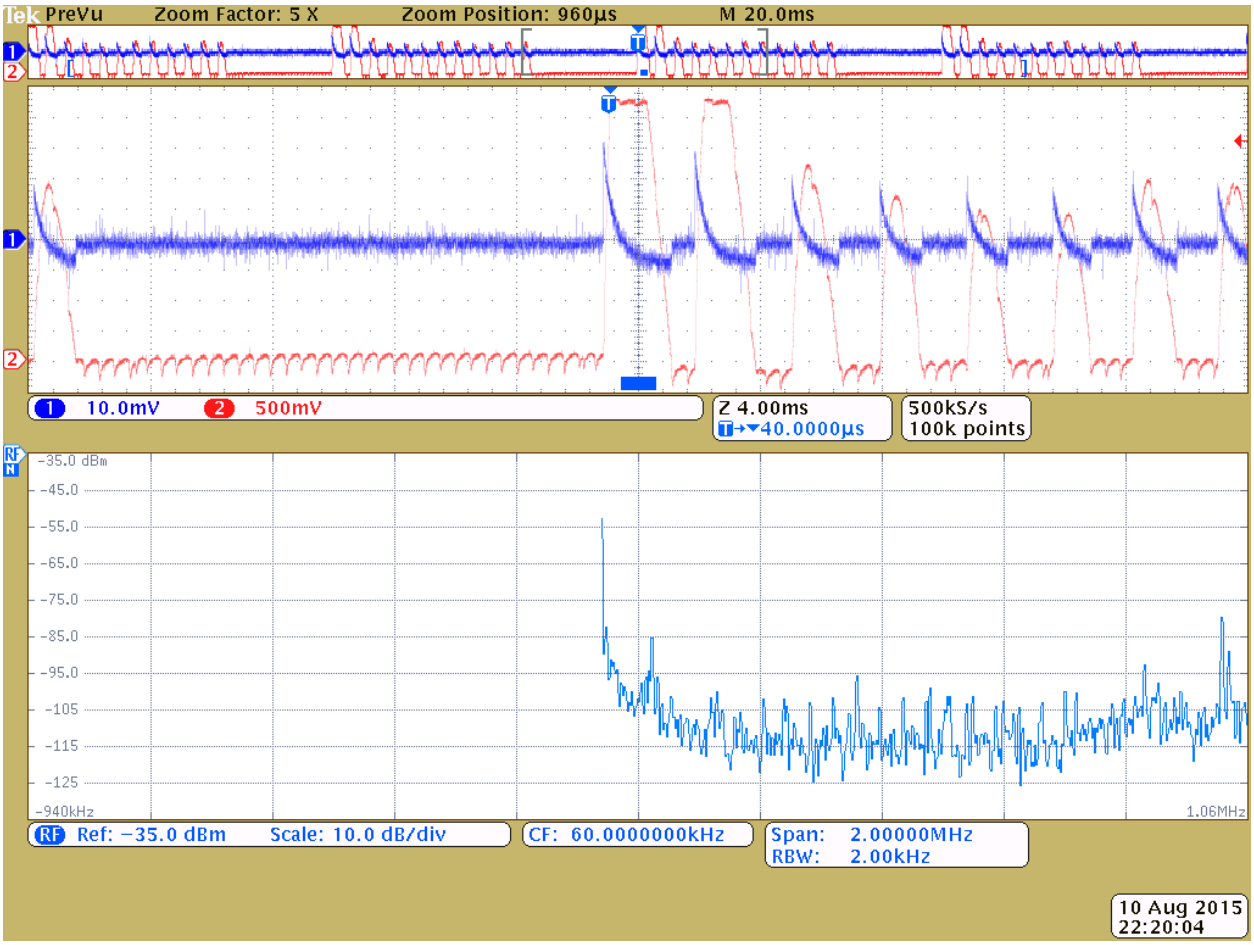

Fig. 2 B Colors and traces as shown in Fig. 2 A. The blue bar of the middle panel is shifted to include the pulse peak and initial shut off of the PECS current. From the peak at about 12 kHz in Fig. 2 a drop of 45 dBm is observed.

Fig. 3 Two nickel specimens 2.5 gm each of 150 mesh fine powder, 99.96 % pure. Temperatures are measured in the die. The temperature profile is the same: 10 min @ 100 A current, 1 min @ 300 A, and 10 min @ 100 A. The cool down is shown at 0 A current.

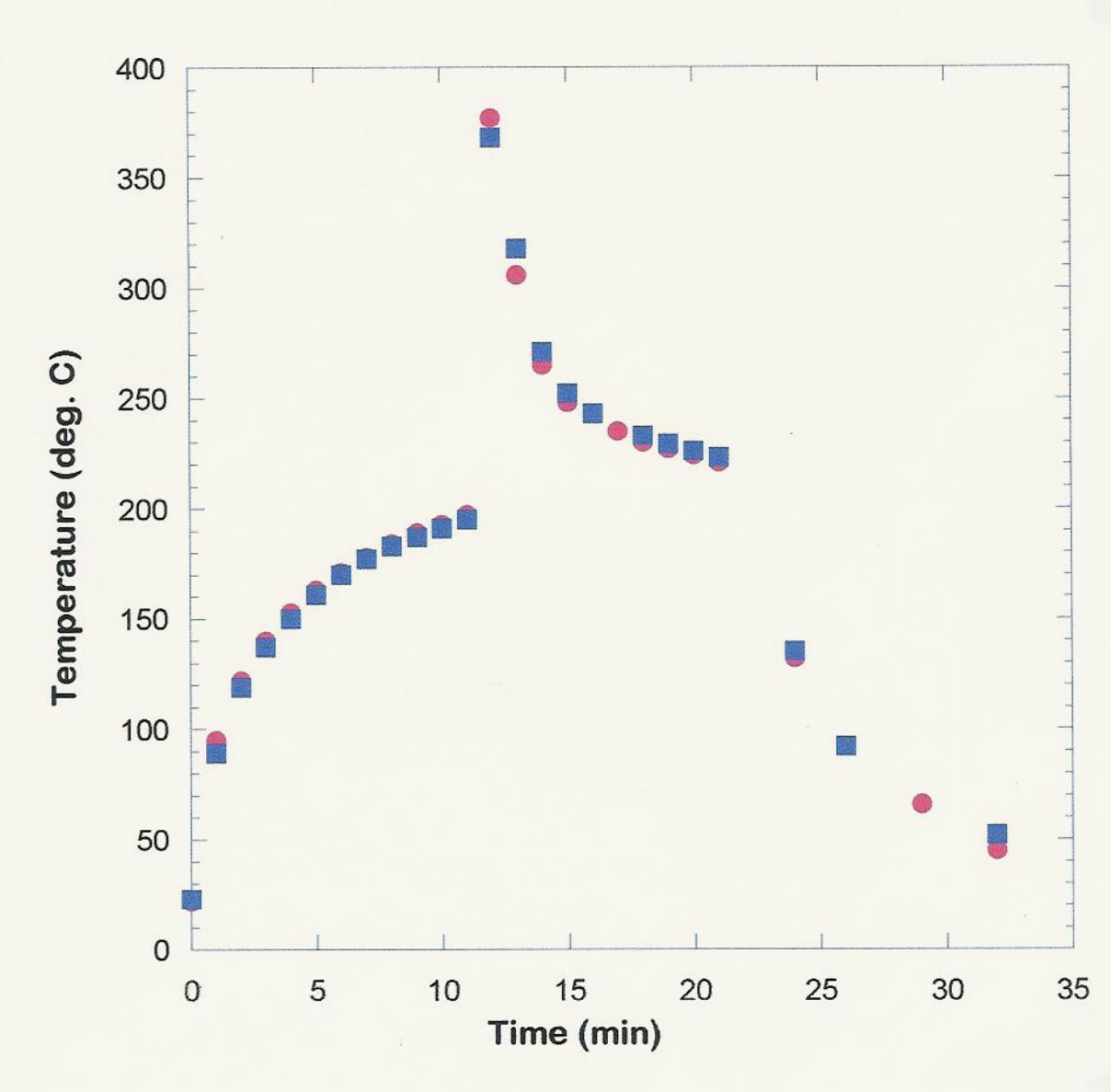

Fig. 4 Temperature measured in the die for two Ni specimens with no disks (red circles & blue squares) and two Ni specimens with Al_2O_3 disks top and bottom of the specimen (black xs & green diamonds).

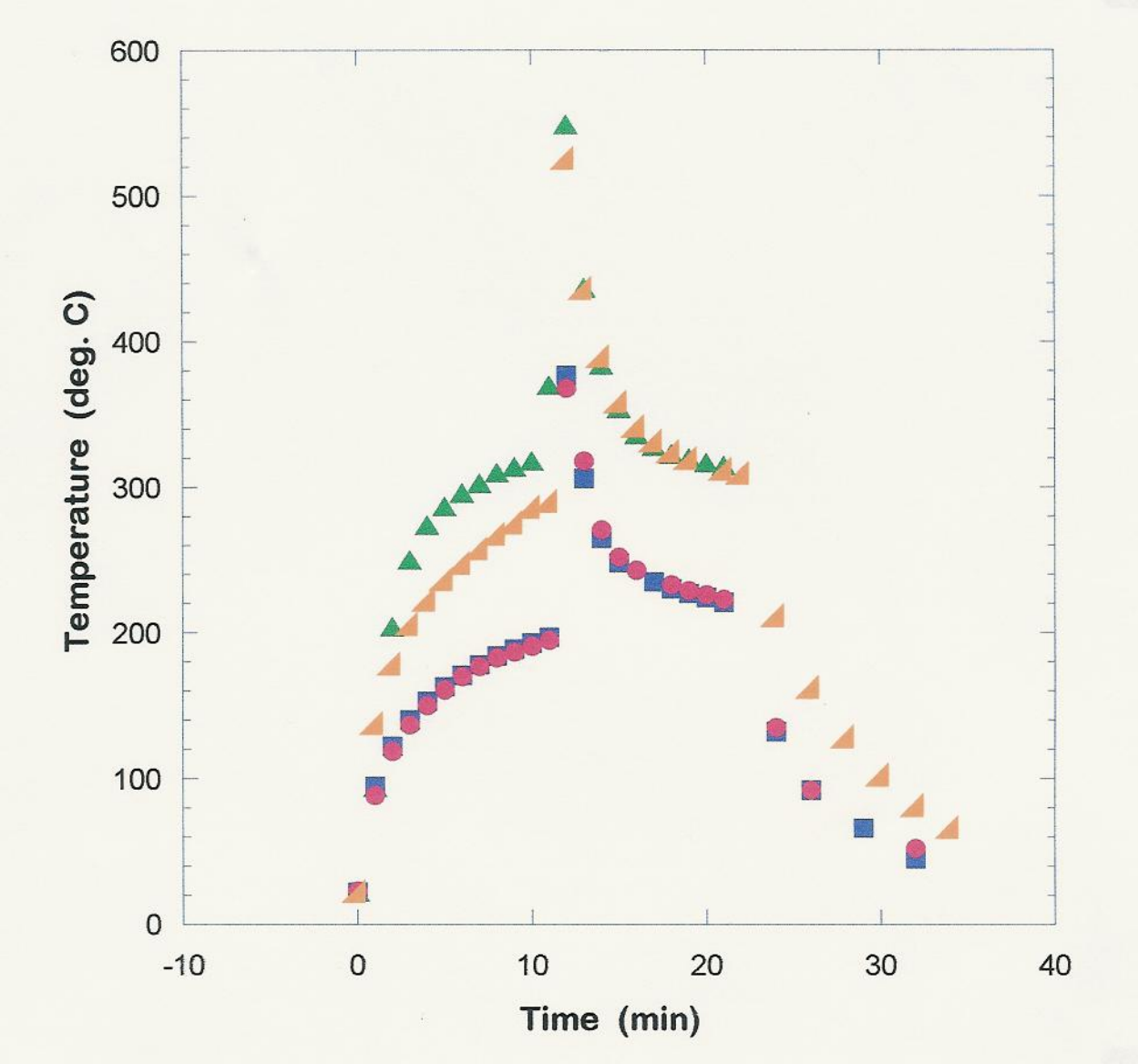

Fig. 5 Mn sintered at 100 A current pulses with and without the Al2O3 disks to limit current pulses though the specimen. The expanded scale shows just the first 10 min but the current profile was the same as for the Ni specimens. The temperature was measured in the die.

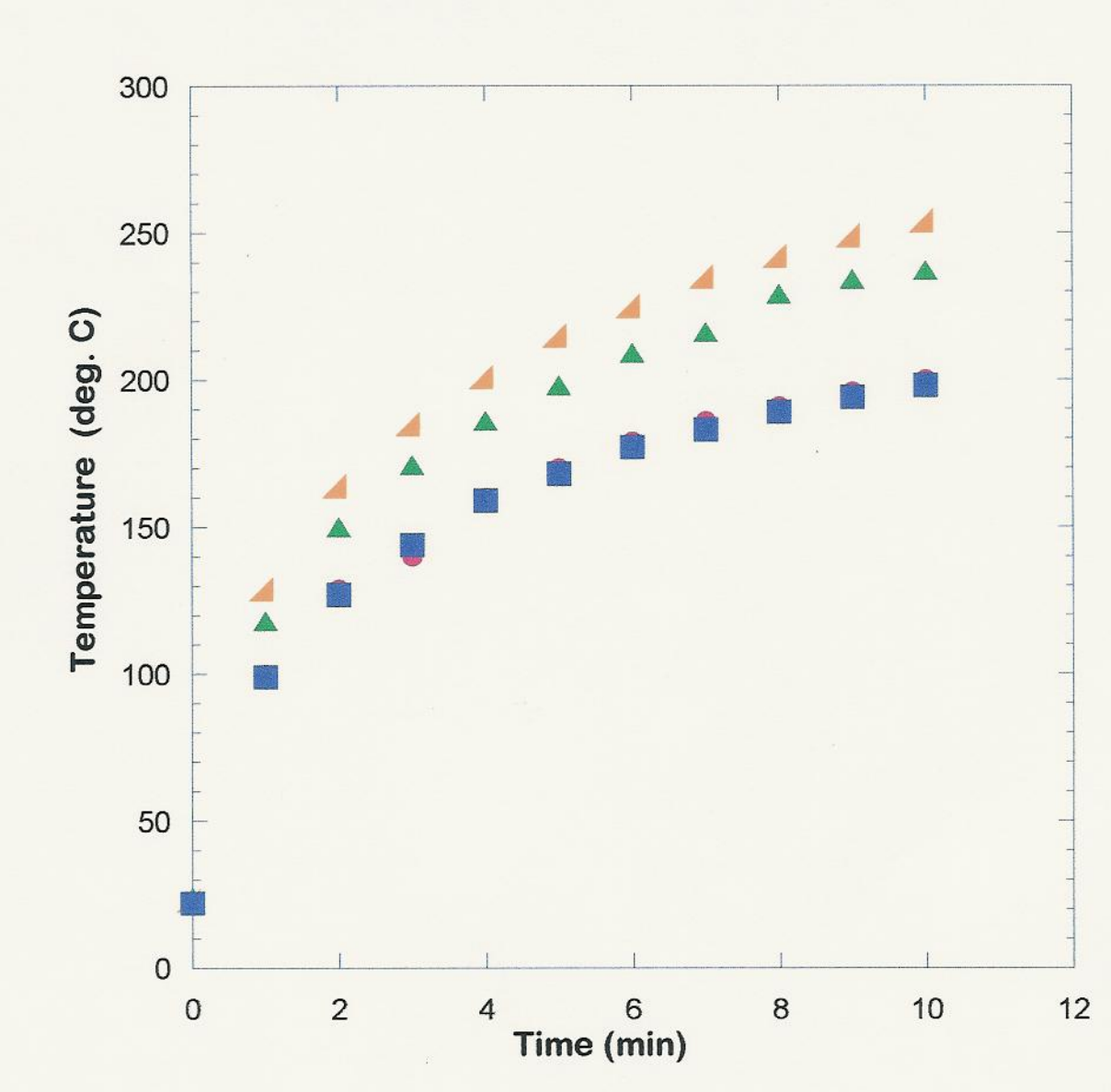

Table I Properties of the specimens used in this report including graphite properties of the punch and die.

Material	$\rho_{electrical}$ Ω-m x 10^{8}	$k_{thermal}$ $Wcm^{-1}K^{-1}$	Melting T ^{o} C	Density gm cm^{-3}	Specific Heat J $mole^{-1}K^{-1}$	
Ni	9.1	0.91	1455	8.9	26.5 20^{o}C	
Mn	144	0.078	1246	7.3	26.1 20^{o}C	
Al_2O_3	$>10^{12}$	0.25	1200 trans.	3.7	79.5 27 ^{o}C	
C graphite	1,500	0.0018-0.013		0.47 – 0.70 100 – 20 mesh	8.52	

Table 2 X-ray line FWHM and sintered density of Ni and Mn specimens with and without Al_2O_3 disks.

Ni	Density (g/cm^3)	FWHM of (011) peak	with Al_2O_3 disks
0915-Ni	6.59	0.255	Yes
0728-Ni	6.10	0.357	Yes
0803-Ni#1	7.77	0.237	No
0803-Ni#2	8.20	0.228	No
Mn	Density (g/cm^3)	FWHM of (221) peak	with Al_2O_3 disks
0713-Mn#3	5.90	0.242	Yes
0713-Mn#4	5.98	0.247	Yes
0721-Mn#1	6.02	0.238	No
0721-Mn#2	6.30	0.214	No
0728-Mn#1	6.28	0.227	No
0728-Mn#2	6.27	0.212	No

ACKNOWLEDGEMENTS

We thank Professor Terry Tritt for the use of the Dr. Sinter™ and his support of this study. Y.F.L. and D.H.L. acknowledge the support of NSF DMR 1307740 and discussions with Dr. Jian He. We thank Dr. Dale Hitchcock and Mr. Roger Livingston who participated in the study of the frequency spectrum of the rf emission using the Tekronix instrument on loan from the Savannah River DOE facility.

References

1. D. Hulbert et al., "The absence of plasma in "spark plasma sintering", J. Appl. Phys. 104, 033305 (2008).

2. Dale Hitchcock, Roger Livingston, Donald Liebenberg, "Improved understanding of the spark plasma sintering process" J. Appl. Phys. 117, 174505 (2015).

3. Dr. Sinter SPS-515S made by Fuji Electronic Industrial Co.

4. S. Lefeuvre, E. Fedorova, O. Gomonova, and J. Tao, "Microwave Sintering of Micro- and Nano-Sized Alumina Powder" **ADVANCES IN MODELING OF MICROWAVE SINTERING** 12th Seminar *Computer Modeling in Microwave Engineering & Applications*, Grenoble, France, March 8-9, 2010, pp 46-50.

5. The Tektronix MDO4104B-6 instrument permits four individual voltage inputs to the oscilloscope and a separate input for the rf signal captured during the same measurement. The power of the rf signal in dB_M has a value $P = 10E(dB_M/10)$ mW.

6. The thermocouple antenna (TCa) was previously demonstrated (see Ref. 2) to detect sparks from a small arc welder. The TCa was used outside the vacuum to detect FM radio signals to 100 MHz including measurement to 1 GHz with the Tektronix MDO410B-6 instrument.

7. CPCO-500 BP-10 Hall current probe by GMW Assoc. San Carlos, CA has an output of 16 mV/A. The response time is stated to be less than 10 μs.

8. B.D. Cuility and S.R. Stock, "Elements of X-Ray Diffarction", 3rd Ed., Prentice-Hall Inc., 2001, p 167-171